Paper pa02-073
Submitted to the 28th International Conference on High Energy Physics
ICHEP'96, Warsaw, Poland, July 1996

# Properties of Transverse Energy Production in Deep-Inelastic Scattering and Comparisions to Monte Carlo Models

H1 Collaboration

**Abstract**

Measurements of observables based on transverse energy are presented for deep-inelastic scattering events produced in positron-proton collisions at HERA. The kinematic range covers squared momentum transfers ($Q^2$) from 2.5 GeV$^2$ to 100 GeV$^2$ and Bjorken $x$ down to $3 \cdot 10^{-5}$. The transverse energy flow is measured for rapidities between $-1 < \eta^* < 6$ in the hadronic center of mass frame. The average transverse energy in a central rapidity bin of $-0.5 < \eta^* < 0.5$ is found to rise, at fixed $Q^2$, with decreasing $x$. The standard Monte Carlo models available describe the gross features of the data. The distribution of the transverse energy in the central rapidity bin has been determined. Transverse energies up to 20 GeV are observed in the data. In addition, energy-energy correlations are presented in the laboratory frame. The growing importance of higher order QCD processes when going towards low $x$ and $Q^2$ is seen.

# 1 Introduction

The large center of mass energy ($\sqrt{s} \approx 300$ GeV ) available at HERA provides for deep-inelastic scattering (DIS) a new QCD testing ground in a regime where the parton momentum fraction $x$ is small, but the transfered momentum squared $Q^2$ large enough to allow perturbation theory to make predictions. Moreover, HERA offers a unique possibility to study events where a large phase space for hadron formation is available but which have momentum transfers down to such low values that non-perturbative phenomena are expected to become dominant.

The inclusive electron measurement revealed a rise of the structure function $F_2$ with decreasing $x$ [1] and has stimulated an exciting discussion on the underlying parton dynamics. However, it is now commonly accepted that the conventional DGLAP evolution equations [2] are sufficient to describe an inclusive observable like $F_2$ down to very low values of $x$ and $Q^2$ (see e.g. [3]).

The multi-purpose HERA detectors allow to measure in addition to the scattered electron a large part of the hadronic final state. Provided that the transition from partons to hadrons can be controlled, this opens the possibility to study the parton dynamics using exclusive observables built on single particle spectra, jets or energy depositions. Variables based on the hadronic final state can be defined for specific rapidity ranges and are therefore well suited to investigate rapidity regions as close as possible to the proton remnant. Furthermore they allow to explore the transition towards the proton remnant starting from the relatively well understood region where the hard subprocess induced by the photon virtuality has taken place.

One of the simplest of such observables is the flow of the transverse energy ($E_T$ ) as function of the rapidity[1] $\eta^*$ in the hadronic center of mass frame. We have measured this observable in the kinematic range of $3 \cdot 10^{-5} < x < 10^{-2}$ and $2.5 < Q^2 < 100$ GeV$^2$ . Furthermore we study the mean transverse energy integrated in the central rapidity bin of $-0.5 < \eta^* < 0.5$ at fixed $Q^2$ as function of $x$ and the transverse energy distribution as a possible inclusive measure of the parton activity near the proton.

Finally, we present transverse energy-energy correlations determined in the laboratory frame.

# 2 Monte Carlo models

A simulation of the detailed properties of the hadronic final state is available in form of Monte Carlo event generators. They usually include the hard subprocess, QCD radiation effects and model the non-perturbative transition from partons to hadrons. They predict the behaviour of a given observable under different approximating assumptions and allow to estimate the validity of comparisons of data to analytical calculations.

The LEPTO Monte Carlo [4] incorporates the QCD matrix element to first order and takes higher order parton emissions approximately into account using the concept of parton showers [5] based on the allowed branching processes of quark and gluons described

[1] Here and throughout this paper the particle masses are neglected such that the pseudo-rapidity $\eta = -\ln\tan(\theta/2)$ coincides with the rapidity.

by the leading log DGLAP equations. The QCD radiation can occur before and after the hard subprocess. The formation of hadrons is performed using the LUND string model [6]. The HERWIG Monte Carlo [7] only differs in details from the above described QCD treatment and relies on leading log parton showers with addional matrix element corrections [8]. It however implements an alternative fragmentation model [9]. ARIADNE [10] calculates the first order matrix element. Higher orders are taken into account by emitting gluons from a chain of independently radiating dipoles spanned by colour connected partons [11]. Hadronizing the partonic state is done by the LUND string model. The DJANGO Monte Carlo [12] is the only event generator which includes the full electroweak matrix element. When DJANGO is used in this analysis, the hadronic final state is modeled by the colour dipole model.

# 3 Detector description

A detailed description of the H1 apparatus can be found elsewhere [13]. The following briefly describes the components of the detector relevant to this analysis.

The hadronic energy flow is mainly measured by the liquid argon (LAr) calorimeter extending over the polar angular range $4.4^\circ < \theta < 153^\circ$ with full azimuthal coverage. The polar angle $\theta$ is defined with respect to the proton beam direction ($+z$ axis). It consists of an electromagnetic section ($20-30$ radiation lenghts) with lead absorbers and a hadronic section with steel absorbers. The total depth of both calorimeters varies between 4.5 and 8 interaction lengths.

Test beam measurements of the LAr calorimeter modules show an energy resolution of $\sigma_E/E \approx 0.50/\sqrt{E\,[\mathrm{GeV}]} \oplus 0.02$ for charged pions. The absolute scale of the hadronic energy is presently known to 5%, as determined e.g. from studies of the transverse momentum balance in DIS events.

The scattered electron is detected by an electromagnetic lead-scintillator calorimeter (BEMC) with a depth of 22.5 radiation lengths covering the backward region of the detector, $151^\circ < \theta < 177^\circ$. The energy scale for electrons is known to an accuracy of 1%.

The calorimeters are surrounded by a superconducting solenoid providing a uniform magnetic field of 1.15 T parallel to the beam axis in the tracking region.

Charged particle tracks are measured in two concentric jet drift chamber modules (CJC), covering the polar angular range $15^\circ < \theta < 165^\circ$. A backward proportional chamber (BPC) with an angular acceptance of $155.5^\circ < \theta < 174.5^\circ$ serves to identify electrons. Using information from the BPC and the reconstructed event vertex the polar angle of the scattered electron is known to better than 5 mrad.

A scintillator hodoscope situated behind the BEMC is used to veto proton-induced background events based on their early time of arrival compared with that for nominal electron-proton collisions.

# 4 Event selection

The data are collected in 1994 with positrons of energy $E_e = 27.5$ GeV colliding on protons of $E_p = 820$ GeV and correspond to an integrated luminosity of 2.7 pb$^{-1}$. The

accessible kinematic range is extended by a dedicated run period where the nominal vertex position was shifted by about 67 cm towards the proton direction. This data sample corresponds to an integrated luminosity of 58 $\mathrm{nb}^{-1}$.

The event kinematics is determined using the information on the scattered electron energy ($E'_e$) and its polar angle ($\theta'_e$) via $Q^2 = E_e E'_e \cos^2(\theta'_e/2)$ and $y = 1 - (E'_e/E_e)\sin^2(\theta'_e/2)$. The variable $x$ is then given by $x = Q^2/ys$. The squared invariant mass of the total hadronic final state can be approximately expressed by $W^2 \approx Q^2(1-x)/x$ . When splitting up the kinematic plane in several slices in $x$ and $Q^2$, the bin sizes are adapted to the resolution of the kinematic variables such that migration between the bins are well under control. DIS events are selected in the following way:

- The energy of the scattered electron has to exceed 12 GeV and its polar angle should be within $157° < \theta'_e < 173°$ for the nominal vertex and within $164° < \theta'_e < 176°$ for the shifted vertex data sample. The radial distance between the energy deposition in the BEMC and the required reconstructed BPC space point has to be smaller than 4 cm. The radial distance of the BPC space point has to lie between 15 and 60 cm ensuring full containment of the electromagnetic cluster.

- The longitudinal momentum balance should be within $30 < \sum_i E_i - P_{z_i} < 70$ GeV, where the sum runs over all energy depositions in the BEMC and LAr calorimeter including the scattered electron.

- There has to be a reconstructed event vertex within $\pm 25$ cm around the mean vertex position.

- The squared invariant hadronic mass as determined from the electron ($W_e^2$) and the hadronic final state alone ($W_h^2$) should be larger than 4400 $\mathrm{GeV}^2$ to ensure sufficient hadronic activity in the detector. This cut effectively restricts the $y$ range to $y > 0.05$. It excludes the region of low $y$ where the measurement by the electron is not reliable.

- The sum of all energy depositions between 4.4° and 15° has to exceed 0.5 GeV. This cut removes events with a forward rapidity gap which are usually assumed to stem from diffractive processes and are not included in all Monte Carlo models used in this analysis. Using the standard procedure to identify diffractive events [14], the remaining fraction of events of this type is evaluated to be 2%.

With these cuts the remaining photoproduction contamination is estimated to be less than 3% of the total data sample.

# 5 Transverse energy flow

The measurement of the transverse energy flow is performed in the hadronic center of mass system (cms), that is the rest system of the proton and the exchanged boson. The orientation of the axis has been chosen such that the proton direction defines the negative

$z$ axis. In this reference frame the transverse components of the momenta are either produced by QCD radiation or originate from the transition of partons to hadrons.

The data are corrected bin-by-bin for detector effects and QED radiation using the DJANGO event generator and a full simulation of the H1 detector. The correction applied never exceeds 50%. The corrected transverse energy flow is presented in Fig. 1 as a function of the rapidity $\eta^*$ in various kinematic bins. The data exhibit transverse energies of about $1.5-2$ GeV per unit of rapidity. The amount of $E_T$ only decreases slowly when going from the current region to the proton direction. For $x < 3 \cdot 10^{-4}$ a plateau is formed.

The mean $E_T$ in the central region ($-0.5 < \eta^* < 0.5$) is an inclusive measure of the parton activity between the current region and the proton remnant. Since there is more phase space for parton emission available when $x$ decreases, the mean $E_T$ is expected to rise. This behaviour is observed in the data as is shown in Fig. 2 for 5 different values of $Q^2$ ranging from 3.5 to 65 GeV$^2$.

The transverse energy measurement has a systematic point-to-point error of about 10% due to the QCD model dependence of the correction functions. Differences found when switching from the usually used shower simulation program GEISHA to CALOR contribute 3% to the systematic error. Further systematic effects are the dependence on the method to determine the kinematic variables (3%), the remaining contamination by photoproduction (3%) and the description of the inactive material in front of the calorimeter (2%). In addition there is an uncertainty of 5% on the normalization due to the limited knowledge of the precision of the hadronic energy scale.

The Monte Carlo models provide a good overall description of the measured transverse energy flow and of the mean $E_T$ in the central rapidity region. LEPTO slightly overshoots the data in the current jet region, while HERWIG falls a little bit below. ARIADNE based on the colour dipole model agrees well, but does not produce sufficient $E_T$ in the lowest $Q^2$ slice. Models based on the DGLAP evolution equations like LEPTO or HERWIG need to produce $60-80\%$ of the $E_T$ during the hadronization phase in order to describe the mean $E_T$. They are able to compensate for the different $x$ dependence seen at the parton level (see Fig.2). In these Monte Carlo models parton emission towards the proton direction gets suppressed by imposing a transverse momentum ordering of the partons. This feature is absent in the colour dipole model allowing parton emission in the full available phase space. The rise of the mean $E_T$ is observed when using this QCD model for partons. Although using the same model for hadronization as LEPTO, only 30%-40% of the $E_T$ is produced non-perturbatively. There is moreover no dependence on $x$ and $Q^2$ such that the measured $E_T$ reflects the $E_T$ produced by the partons. An analytical QCD calculation [15] based on the BFKL equations [16] also predicts the same $x$ dependence of the mean $E_T$ as seen in the data (see Fig.2 triangles). This calculation is, however, only carried out for partons. Moreover, QCD radiation of the current jet has been neglected. It is therefore not directly comparable to the data. One can note that it leaves room only for 10%-20% additional $E_T$ .

In a previous analysis [17] the $E_T$ flow in DIS events has been compared to events produced in real photon-proton collisions[2]. For this purpose the invariant mass of the hadronic final state is fixed to $W^2 \approx 180$ GeV$^2$ by requiring $0.3 < y < 0.5$.

[2]In order to directly compare to these results, in this particular analysis diffractive events are not removed. This results in a shift of about 10% on the mean $E_T$.

The transverse energy flow shows quite a similar behaviour for $Q^2$ values of 0, 3.5 and 7 GeV$^2$ for all measured rapidities as is shown in Fig.3. After a rise towards the current region, a plateau of about $1.6 - 1.8$ GeV extending to the last reachable rapidity point al low $\eta^*$ becomes visible. As can be seen in Fig.4, the mean $E_T$ in the rapidity bin $2 < \eta^* < 3$ only starts rising for $Q^2$ around 10 GeV$^2$. Fig.4 also illustrates that the virtuality of the photon has only very little influence on the mean $E_T$ measured in the central rapidity region. An almost constant amount of $E_T$ is measured for $Q^2$ from 0 up to 900 GeV$^2$.

# 6 Transverse energy distribution

The composition of the mean $E_T$ can be revealed by measuring the distribution of the transverse energy. This observable allows to decide if the mean $E_T$ is the result of many small contributions or if a few large $E_T$ values significantly influence the mean. The $E_T$ stemming from hadronization is expected to be limited, while high $E_T$ values are more likely produced by parton activity. The tail of the $E_T$ distribution is therefore an interesting observable to study the underlying parton dynamics.

To control the migrations towards higher $E_T$ values mainly induced by the hadronic energy resolution, the bin sizes are chosen such that more than 50% of the $E_T$ stays in the bin where it was produced. The size of the migrations are determined by comparing generated and reconstructed Monte Carlo events. The data are then corrected for detector acceptance and resolution by a bin-to-bin procedure.

The corrected transverse energy distribution is shown in Fig.5 for 17 bins in the kinematic plane. Transverse energies up to 20 GeV are observed. At fixed $Q^2$ the $E_T$ distribution gets harder if $x$ decreases and at fixed $x$ more $E_T$ is produced for increasing $Q^2$ (see Fig.6). This might be taken as an indication that the underlying parton activity increases, if more phase space is available. The colour dipole model Monte Carlo describes the data in all kinematic regions. The DGLAP based Monte Carlos LEPTO and HERWIG exhibit a softening of the tail when $x$ decreases. As discussed above, these Monte Carlo models produce on average enough transverse energy, but do not seem to be able to account for the large transverse energies seen on a event-by-event basis. The available statistics, however, does not allow strong conclusions to be drawn. The systematic error has not yet been fully evaluated, but is, in the region of high $E_T$, estimated to be small compared to the statistical one.

# 7 Energy-energy correlation

The energy-energy correlation have been a useful tool to study QCD effects in $e^+e^-$ collisions. In DIS events energy-energy correlations are sensitive to hard QCD processes, soft gluon emission and hadronization effects. The measurement is carried out in the laboratory system.

Denoting for each event the transverse energy $E_{T\,i}$, the rapidity $\eta_i$ and the azimuth $\phi_i$ of each energy deposition in the calorimeter or each particle (for Monte Carlo generator data) $i$, a distance between two objects in the $\eta$-$\phi$ plane is constructed by $\omega^2 = (\eta_i -$

$\eta_j)^2 + (\phi_i - \phi_j)^2$. Using the $p^2_{T\,e}$ of the scattered electron as a normalization, the transverse energy-energy correlation at a distance $\omega$ can be defined as

$$\Omega(\omega) \;=\; \frac{1}{N\,\Delta\omega} \sum_N \sum_{i,j;i<j} \frac{E_{T\,i}\,E_{T\,j}}{p^2_{T\,e}} \int_{\omega-\frac{\Delta\omega}{2}}^{\omega+\frac{\Delta\omega}{2}} \delta(\omega' - \omega_{ij})\;\mathrm{d}\omega' \,, \qquad (1)$$

where $\Delta\omega$ is the bin width and the sum is made over objects within the polar acceptance of $4^\circ < \theta < 174^\circ$ and over all $N$ events.

The corrected transverse energy-energy correlations are shown in Fig. 7. Only statistical errors are included in the figure. Note that the statistical errors of the energy-energy correlations are not independent of each other, since each energy deposition contributes many times.

The applied corrections to take detector effects into account were never larger than 50% over the full $\omega$ range shown. Even though no Monte Carlo model perfectly describes the data, they all lead to similar correction functions. The systematic error introduced by the model dependence of the correction procedure is 15%. The uncertainty of the energy scale on the hadronic energy measurement and on the scattered electron results in an overall normalization uncertainty of 12%. The data are not corrected for radiative QED effects. However, due to the restricted $y$ range QED radiation affects the data by less than 2% and mainly changes the overall normalization. Using different methods to reconstruct the event kinematics changes the result by 10%. All these effects sum up to a total systematic error of 21%.

While at large $x$ and $Q^2$ the strongest correlation is seen for nearby transverse energy depositions (low $\omega$), the correlation for back-to-back transverse energy depositions ($\omega = \pi$) becomes stronger when going towards lower $x$ and $Q^2$. This shows the increasing importance of higher order QCD processes towards low $x$ and $Q^2$. None of the available Monte Carlo models is able to fully describe the details of the distribution over the full kinematic plane. The best description is achieved by HERWIG. LEPTO predicts a different shape at large $x$ and $Q^2$. The colour dipole model as implemented in the DJANGO Monte Carlo program falls below the data.

# 8 Conclusion

For deep-inelastic scattering events we have measured the flow of the transverse energy in the rapidity range of $-1 < \eta^* < 6$ in the hadronic center of mass frame for 17 different kinematic bins covering $3 \cdot 10^{-5} < x \; < 10^{-2}$ and $2.5 < Q^2 < 100$ GeV$^2$.

We studied the mean $E_T$ in the central rapidity region $-0.5 < \eta^* < 0.5$ for fixed $Q^2$ as function of $x$. The rise of the mean $E_T$ for decreasing $x$ as predicted by the BFKL equation for partons is seen in the data. However no firm conclusion can been drawn, since the Monte Carlo models incorporating parton showers based on the DGLAP equations are able to compensate the lack of parton activity in the central rapidity region by producing a large amount of $E_T$ in what they call the hadronization phase. The colour dipole Monte Carlo allowing for parton emission in the full available phase space describes the rise of $E_T$ with decreasing $x$ and only needs relatively little non-perturbatively produced additional $E_T$.

Measuring a new point at low $Q^2$ we have verified our previous finding that, for fixed $W^2$, the mean $E_T$ in the rapidity region of $2 < \eta^* < 3$ is constant for $Q^2$ values ranging from 0 GeV$^2$ to about 10 GeV$^2$ . We observe furthermore that the mean $E_T$ produced in the central rapidity region does almost not depend on the virtuality of the photon inducing the hard scattering.

We have evaluated the $E_T$ distribution in the central rapidity region in the full kinematic plane. Transverse energies up to 20 GeV are present in the data. The observed hard tail gets more pronounced with decreasing $x$ at fixed $Q^2$ and with increasing $Q^2$ at fixed $x$ . The data are well described by the colour dipole Monte Carlo model. While the DGLAP based Monte Carlo models HERWIG and LEPTO agree with the data at large $x$ and $Q^2$ they show, compared to the data, a softening of the transverse energy tail when going (at fixed $Q^2$) towards lower values of $x$. However, no firm conclusions can be drawn from the present statistics.

The energy-energy correlations in the laboratory system have been measured in the full available kinematic range. At high $x$ and $Q^2$ this distribution exhibits a peak at low values of the distance measure $\omega$ ($\omega^2 = \Delta\eta^2 + \Delta\phi^2$) induced by near-by particles. When going to lower values of $x$ and $Q^2$ a strong correlation develops at values of around $\pi$ indicating that higher order QCD processes get more and more important. The Monte Carlo models follow the gross features of this distribution, but no model is able to fully describe the details in all kinematic bins.

# Acknowledgments

We are grateful to the HERA machine group whose outstanding efforts have made and continue to make this experiment possible. We thank the engineers and technicians for their work in constructing and now maintaining the H1 detector, our funding agencies for financial support, the DESY technical staff for continual assistance, and the DESY directorate for the hospitality which they extend to the non-DESY members of the collaboration.

# References

[1] H1 Collab., S. Aid et al., Nucl.Phys. B470 (1996) 3; ZEUS Collab., M. Derrick et al., Z. Phys. C69 (1996) 607.

[2] Yu. L. Dokshitzer, Sov. Phys. JETP 46 (1977) 641; V.N. Gribov and L.N. Lipatov, Sov. J. Nucl. Phys. 15 (1972) 438 and 675; G. Altarelli and G. Parisi, Nucl. Phys. 126 (1977) 297.

[3] H1 Collab., S. Aid et al., Nucl.Phys. B470 (1996) 3.

[4] G. Ingelman, *in* Proc. HERA workshop, Eds. W. Buchmüller and G. Ingelman, Hamburg (1991) Vol. 3, 1366. G. Ingelman, A. Edin and J. Rathsman, DESY-preprint 96057, Hamburg, April 1996 and hep-ph/9605286, Version used: 6.4

[5] M. Bengtson, T. Sjöstrand, Z. Phys. C37 (1988) 465; M. Bengtson, G. Ingelman, T. Sjöstrand, Proc. of the HERA Workshop 1987, ed. R.D. Peccei, DESY Hamburg 1988, Vol. 1, p149.

[6] T. Sjöstrand, Computer Phys. Comm. 39 (1986) 347;
T. Sjöstrand and M. Bengtsson, Computer Phys. Comm. 43 (1987) 367, and for JETSET 7.3, T. Sjöstrand, CERN-TH-6488-92 (1992); CERN-Th 7112/93 Dec. 93

[7] G. Marchesini et al., Computer Phys. Comm. 67 (1992) 465. Version used: HERWIG 5.8.

[8] M. Seyour, Nucl. Phys. B436 (1995) 443.

[9] B.R. Webber, Nucl. Phys. B238 (1984) 492.

[10] L. Lönnblad, Computer Phys. Comm. 71 (1992) 15. Version used: ARIADNE 4.8.

[11] G. Gustafson, Ulf Petterson, Nucl. Phys. B306 (1988); G. Gustafson, Phys. Lett. B175 (1986) 453; B. Andersson, G. Gustafson, L. Lönnblad, Ulf Petterson, Z. Phys. C43 (1989) 625.

[12] G.A. Schuler and H. Spiessberger, Proceedings of the Workshop Physics at HERA, W. Buchmüller and G. Ingelman (editors), October 1991, DESY-Hamburg) vol.3 p. 1366. Version used: DJANGO 6.

[13] H1 Collab., I. Abt et al., DESY internal report, H1-96-01 (1996), submitted to Nucl. Instr. and Meth..

[14] H1 Collab., T. Ahmed et al., Phys. Lett. B348 (1995) 681.

[15] K. Golec-Biernat, J. Kwieciński, A.D. Martin and P. Sutton, Phys. Lett.B335 (1994) 220, and P. Sutton private communication.

[16] E.A. Kuraev, L.N. Lipatov and V.S. Fadin, Sov. Phys. JETP 45 (1972) 199; Y.Y. Balitsky and L.N. Lipatov, Sov. J. Nucl. Phys. 28 (1978) 282.

[17] H1 Collab., S. Aid et al., Phys. Lett. B356(1995)118

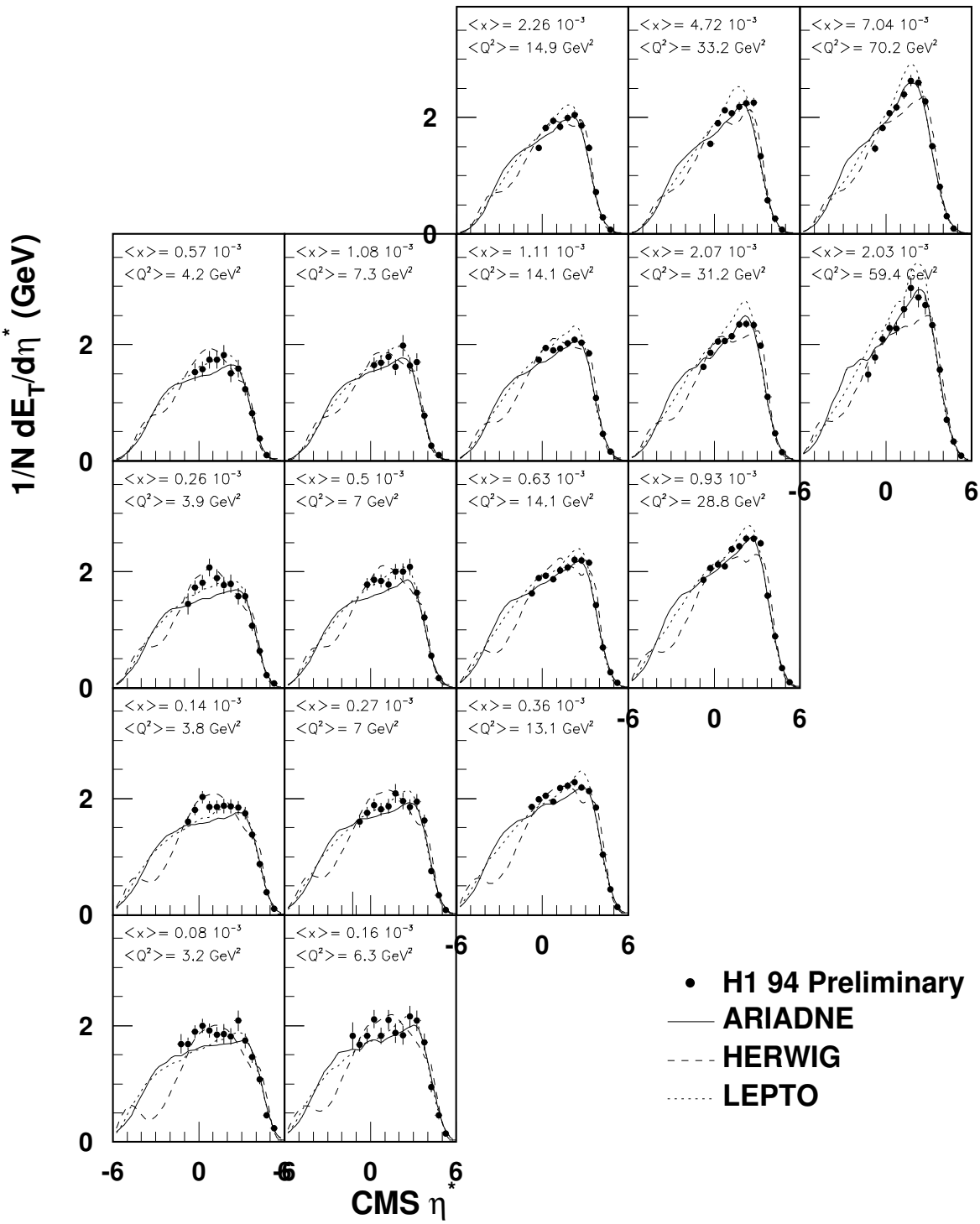


Figure 1: *Transverse energy flow measured in the hadronic center of mass frame as function of the rapidity $\eta^*$ for various bins in $x$ and $Q^2$. The points indicate the* H1 *data, shown are only statistical errors. The lines are the Monte Carlo predictions for the colour dipole model (solid line), HERWIG (dashed line) and LEPTO (dotted line). The proton direction points to the negative $z$ axis.*

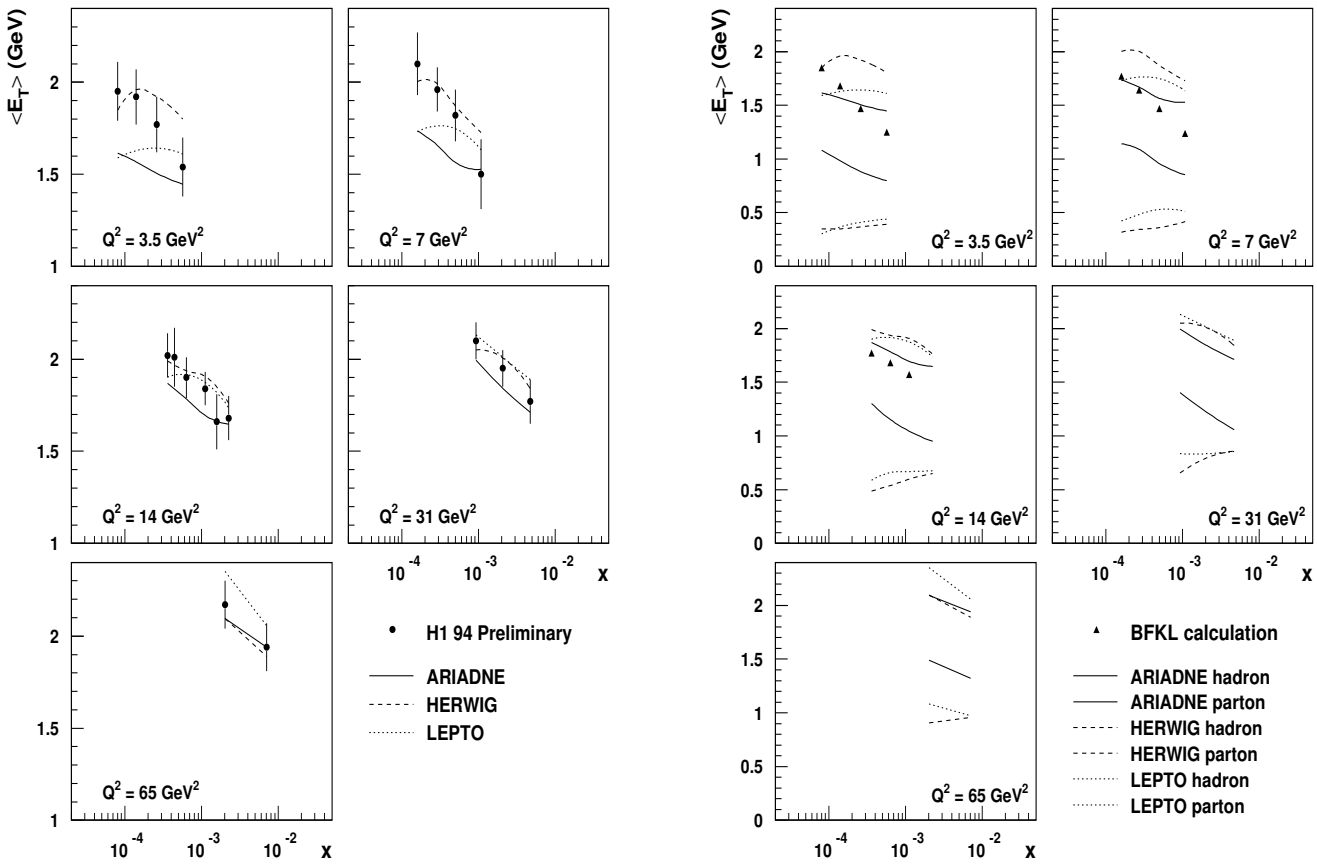


Figure 2: *Left: Mean transverse energy in the central rapidity bin* $-0.5 < \eta^* < 0.5$ *at fixed* $Q^2$ *as function of* $x$*. The points show the H1 data, statistical and systematic errors are added in quadrature. An additional error affecting only the overall normalization introduced by the errors on the energy scales of* $8\,\%$ *is not included in the figure. The curves are the Monte Carlo prediction from the colour dipole model (solid line), HERWIG (dashed line) and LEPTO (dotted). Right: The prediction of an analytical BFKL calculation carried out for partons for the mean* $E_T$ *in function of* $x$ *(triangles). Shown are as well the curves obtained from Monte Carlo event generators on parton (lower curve) and hadron (upper curve) level.*

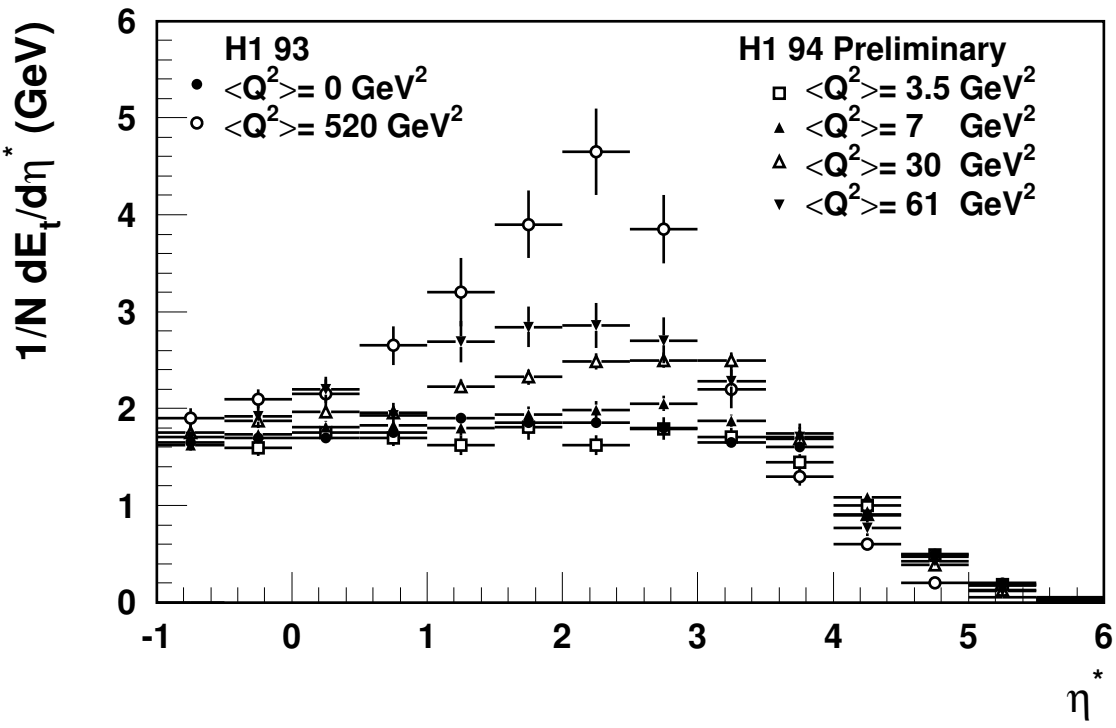


Figure 3: *Transverse energy flow as function of the rapidity $\eta^*$ in the center of mass frame at fixed $W^2 \approx 180$ GeV$^2$ for different values of $Q^2$ ranging from 0 to 520 GeV$^2$ . Shown are statistical errors only. The proton direction points to the negative z axis.*

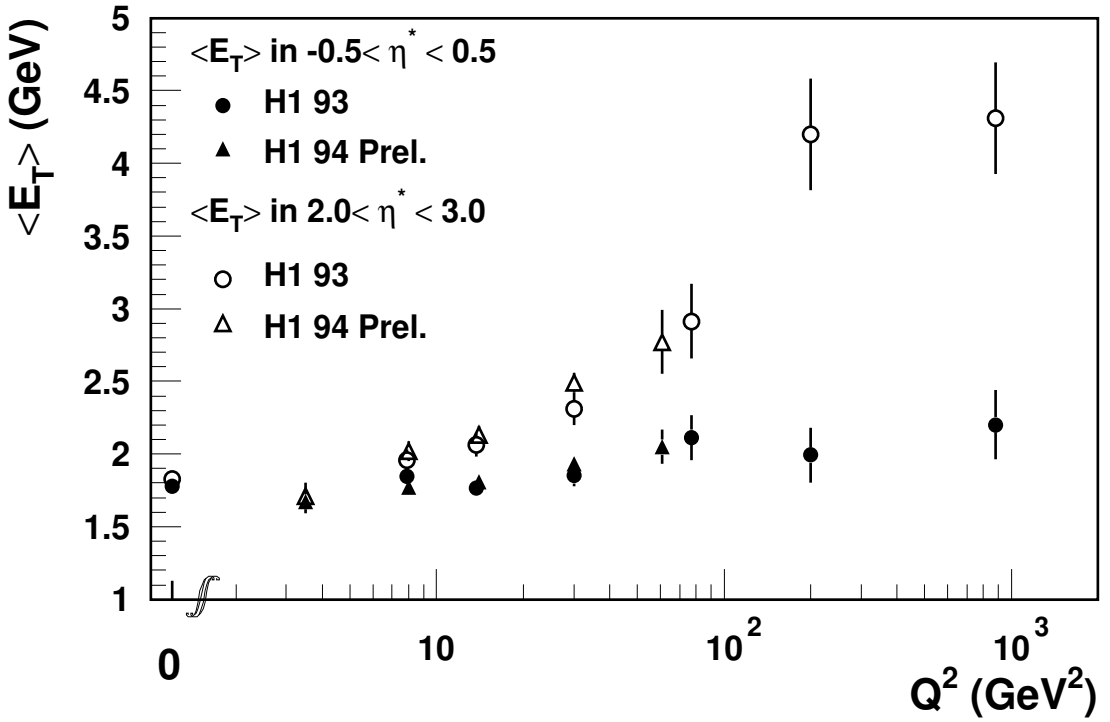


Figure 4: *Mean transverse energy in two different bins of rapidity $\eta^*$ as function of $Q^2$. Shown are only the statistical errors.*

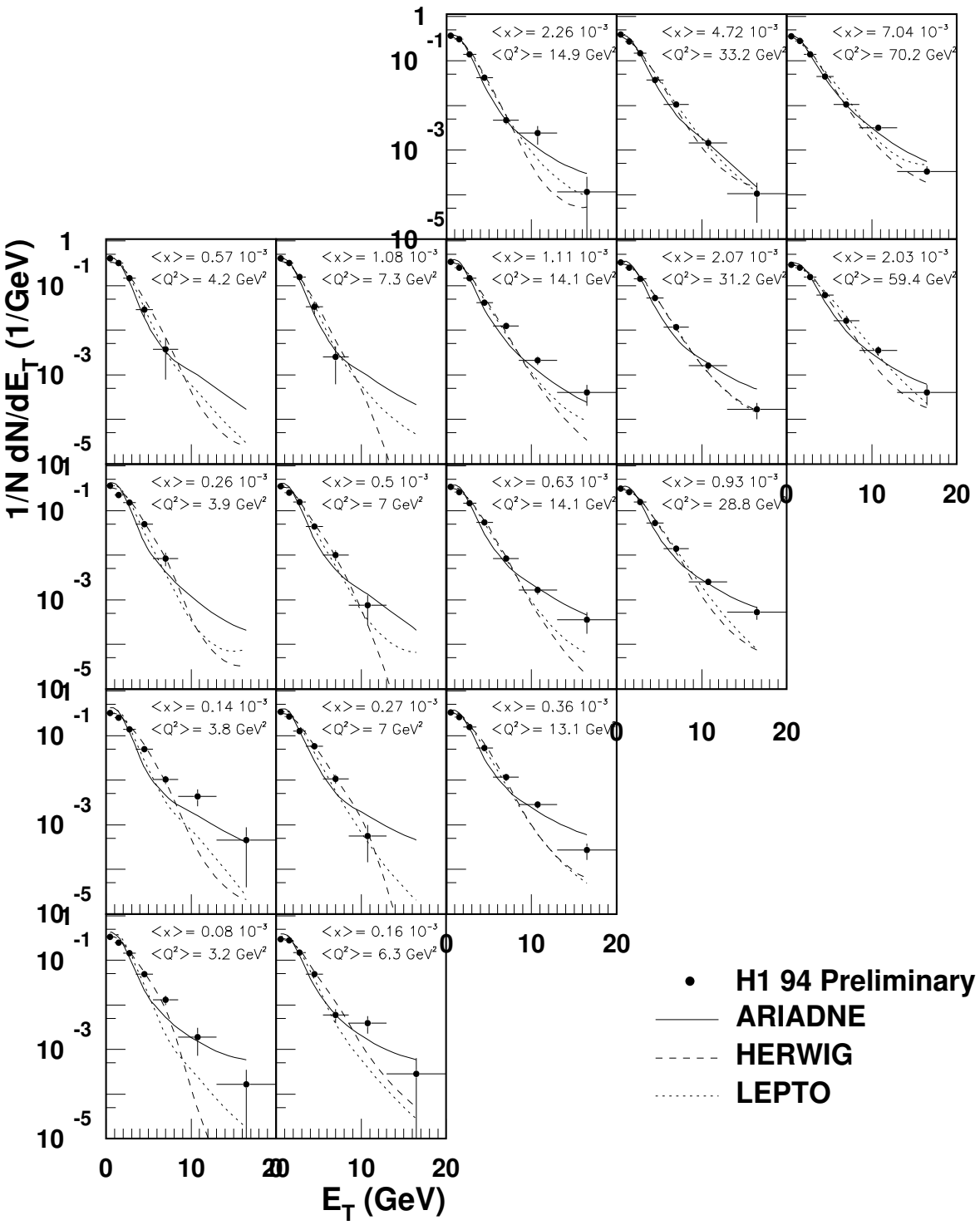


Figure 5: *Transverse energy distribution in various bins of $x$ and $Q^2$. The points indicate the H1 data. Shown are only statistical errors. Superimposed are the predictions from different Monte Carlo models: the colour dipole model (solid line), HERWIG (dashed line) and LEPTO (dotted line).*

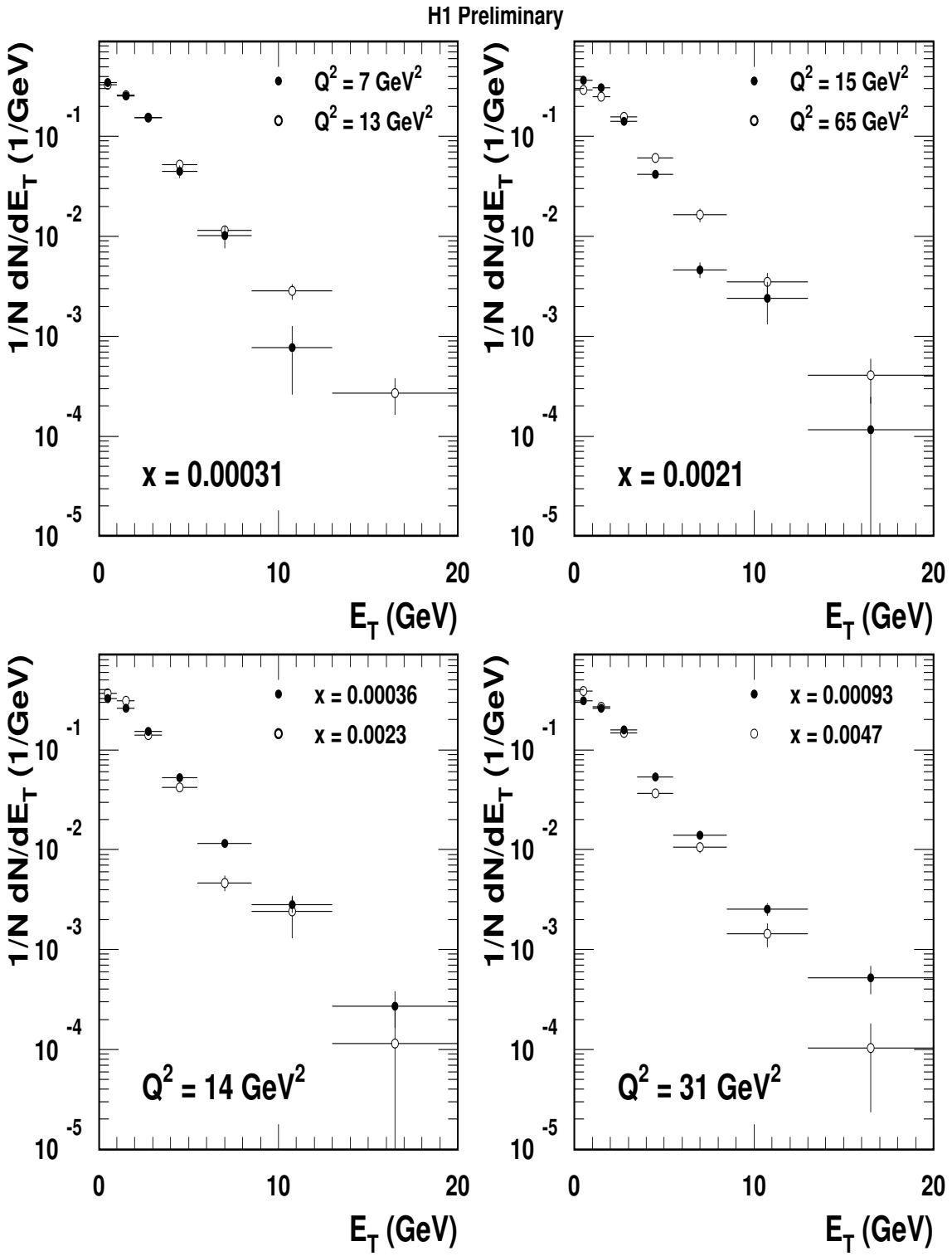


Figure 6: *Transverse energy distribution for fixed $x$ and two different $Q^2$ values and for fixed $Q^2$ for two different $x$ bins. Only statistical errors are included in the figure.*

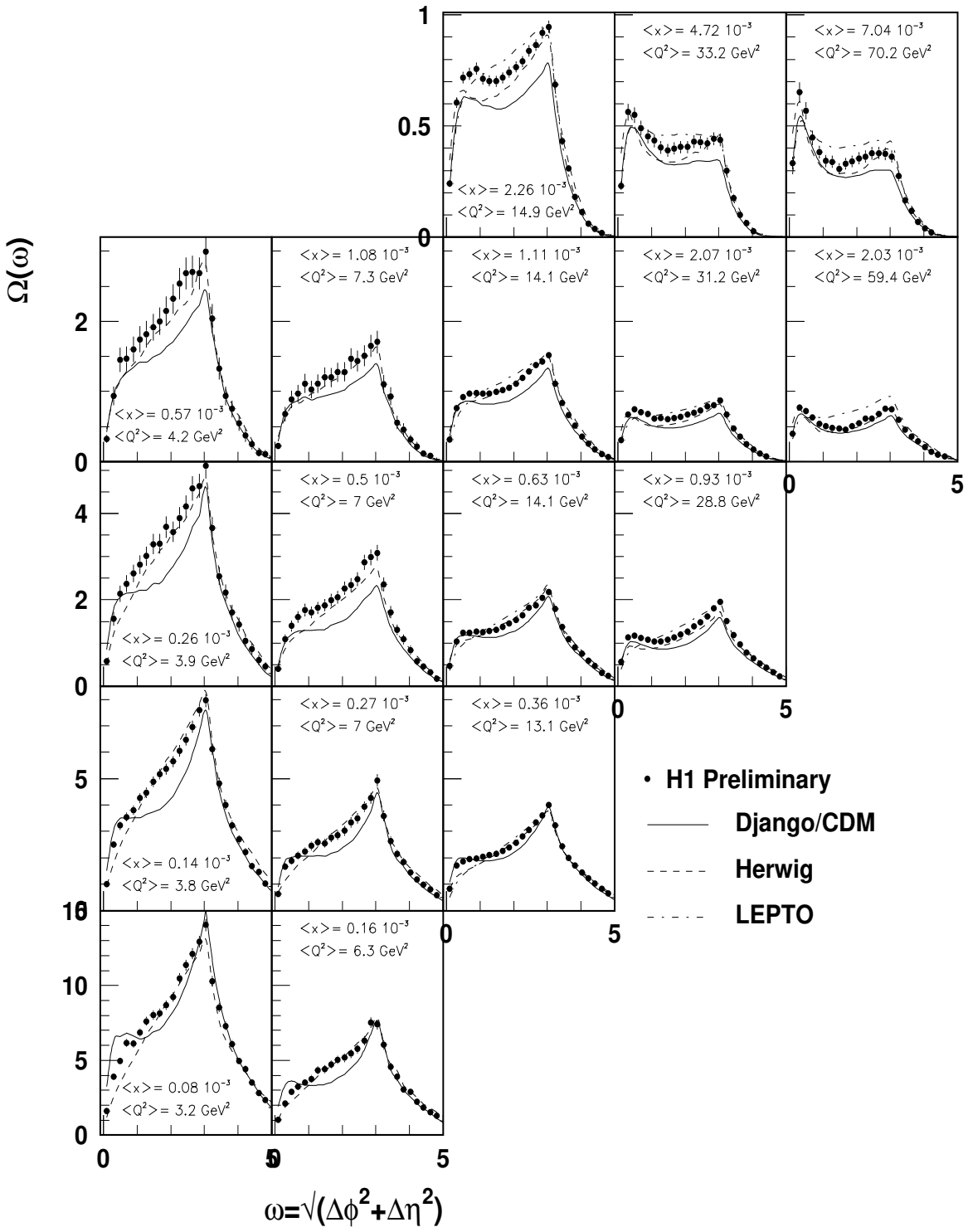


Figure 7: *Transverse energy-energy correlations measured in the laboratory system as function of the distance measure $\omega$ in various bins of $x$ and $Q^2$. The points indicate the data. Shown are only statistical errors. The curves are the prediction from the Monte Carlo models: DJANGO/CDM (solid line), HERWIG (dashed line) and LEPTO (dashed dotted line). The LEPTO curve is only shown for $Q^2 > 10$ GeV$^2$ .*